

# Comparison between electrochemical capacitors based on NaOH and KOH activated carbons

*Silvia Roldán, Isabel Villar, Vanesa Ruíz, Clara Blanco, Marcos Granda, Rosa Menéndez, Ricardo Santamaría\**

Instituto Nacional del Carbón (CSIC), P.V. Box 73, 33080-Oviedo (Spain)

\* Corresponding author. E-mail : [riqui@incar.csic.es](mailto:riqui@incar.csic.es)

**Abstract.** This work describes the chemical activation of a coke using two different activating agents in order to investigate their behaviour as electrodes in supercapacitors. A coke was chemically activated with two hydroxides (KOH and NaOH) under nitrogen flow, at a constant mass hydroxide/coke ratio of 2 and temperatures of 600, 650 and 700 °C. All the samples were characterized in terms of porosity by N<sub>2</sub> sorption at 77 K, surface chemistry by temperature programmed desorption (TPD) and electrical conductivity. Their electrochemical behaviour as electric double layer capacitors was determined using galvanostatic, voltammetric and impedance spectroscopy techniques, in an aqueous medium with 1M H<sub>2</sub>SO<sub>4</sub> as electrolyte. Large differences in capacitive behaviour with the increase in current density were found between the two series of activated samples. The different trends were correlated with the results obtained from the TPD analysis of the CO-type oxygen groups. It was found that these oxygen groups make a positive contribution to capacitance finding a good correlation between the specific capacitance values and the amount of these oxygen groups was found for both series.

**Keywords.** Coke ; chemical activation ; activation temperature; carbon electrodes ; electrochemical properties; supercapacitors.

## 1. Introduction

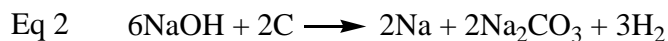
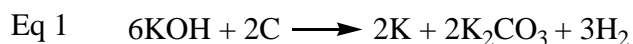
Chemical activation is now considered as an efficient technique for preparing microporous active carbons. Several advantages make it better than physical activation for this purpose, namely: it is a single-step process, high burn-offs can be reached in a short time, it gives rise very high specific surface areas and a well-developed microporosity with a controlled micropore size distribution. However, chemical activation shows some disadvantages of chemical activation process, such as the corrosiveness of the process and the washing stage<sup>1</sup>.

Among the classical reagents which can be used for chemical activation<sup>2</sup>, alkali hydroxides seem to be those in which the microporosity of the as-prepared materials is the most developed. For this reason, the number of studies related to the preparation of activated carbons by chemical activation with KOH<sup>3-7</sup> and, more recently, with NaOH<sup>3,5,7,8</sup> is increasing. This last hydroxide, an activating agent scarcely referred to the literature, has some advantages over KOH. The most important are its low price, simple handling procedure and less corrosive behaviour, all of which are of interest especially from an industrial point of view.

It has been shown<sup>4</sup> that some experimental variables have a strong influence on the porosity of the activated carbons prepared by chemical activation with hydroxides: the activating agent/carbon ratio, the method of mixing the activating agent and carbon, the temperature and flow of gas during carbonization, etc.

As far as we know, the number of studies that employ NaOH as activating agent is still relatively low. In particular, no detailed study of the effect of heat treatment on the electrochemical properties of the resultant activated carbons has yet been reported. Only studies employing activation with KOH have been published<sup>4</sup>. Even though NaOH and KOH are related compounds, the direct transfer of results from KOH to NaOH activation is not a simple matter. This is because the reaction mechanisms of these two hydroxides are different. KOH intercalates between carbon layers<sup>9</sup>, while NaOH reacts with the most energetic sites of the surface, thus displaying a reactivity which strongly depends on the

aromaticity and cristallinity of the carbonaceous precursor<sup>10-12</sup>. Nevertheless, the overall reactions of these precursors with carbonaceous materials are similar as can be seen from equations Eq 1 and Eq 2<sup>10</sup>.



In the present paper, a coke was activated with KOH and NaOH following a procedure in which the only parameter allowed to vary was the temperature of activation. The objective of this work is to study the effect of temperature on the resultant activated materials in order to compare and optimize their behaviour as electrodes of supercapacitors.

## 2. Experimental Section

### 2.1. Preparation of the activated carbons

A coke obtained from a coal tar pitch at 500°C for 4 h under nitrogen, with 100 % mesophase content, was used as raw material. It was ground and sieved to a particle size of less than 400 µm. Chemical activation was performed using KOH and NaOH as activating agents. The activated carbons were obtained by means of physical mixing. The coke was mixed, by stirring, with the activating agent (anhydrous NaOH or KOH) at a weight ratio of 1:2. The resulting mixture was then carbonized.

Carbonization was carried out in an electric furnace. The samples were heated (2.3°C.min<sup>-1</sup>) from room temperature, under a nitrogen flow rate of 500 ml.min<sup>-1</sup>, and then kept at different final temperatures (600, 650 or 700 °C), for 1 hour, before being cooling down under nitrogen.

The pyrolyzed samples were washed repeatedly with a 3 M solution of HCl and then with distilled water until a pH of 6.5 were obtained in order to remove chloride ions. Once the activating agent was removed, the resultant materials were dried at 110°C for 24 hours.

The activated carbons produced at the different temperatures were designated as NaOH-600, NaOH-650, NaOH-700, KOH-600, KOH-650 and KOH-700, where the letters refer to the activating agent and the numbers to the carbonization temperature.

## 2.2. Characterization of the activated carbons.

### 2.2.1. Porous texture.

Porous texture characterization was carried out by physical adsorption of nitrogen at 77 K. Isotherms were obtained on an *ASAP 2020 Micromeritics* apparatus using around 50 mg of sample in each experiment. The pores were classified according to IUPAC recommendations<sup>13</sup> into micropores (< 2 nm width), mesopores (2-50 nm width) and macropores (> 50 nm width). The apparent surface area was determined from the N<sub>2</sub>-adsorption isotherm using the BET equation. The total micropore volume (V<sub>N2</sub>) was calculated by applying the Dubinin-Radushkevich equation<sup>14</sup> to the N<sub>2</sub> adsorption isotherms, and the total pore volume was obtained from N<sub>2</sub> adsorption when P/P° = 0.99. The volume of mesopores was calculated by subtracting the total micropore volume (V<sub>N2</sub>) from the total pore volume. The microporous surface area was obtained from the equation:  $S_{mic} (m^2 \cdot g^{-1}) = 2000 V_{N2} (cm^3 \cdot g^{-1})/L_0 (nm)$ , where L<sub>0</sub> represents the average micropore width<sup>15</sup>.

### 2.2.2. Chemical characterization

The activated carbons were characterized by elemental analysis. Carbon, hydrogen, sulphur and nitrogen contents were determined using a LECO-CHNS-932 microanalyzer. The oxygen content was obtained directly using a LECO-TF-900 furnace coupled to the same microanalyzer.

To characterize the surface chemistry of all the samples, temperature programmed desorption (TPD) experiments were performed in a U-shaped quartz cell coupled to a mass spectrometer in order to determine the amount and type of the oxygenated functionalities. In these experiments about 50 mg of sample was heated up to 1000 °C, at a heating rate of 10 °C.min<sup>-1</sup>, under a helium flow rate of 50 mL.min<sup>-1</sup>.

### 2.2.3. Electrical conductivity

The electrical conductivity of the activated samples was determined using a four-point method<sup>16</sup>. Measurements were performed at various pressures up to 40 MPa. These were calculated using a loaded cell for high accuracy.

### 2.3. Electrode preparation and electrochemical characterization

For the electrochemical characterization, disk type electrodes were prepared using 10 wt.% of polyvinylidene fluoride (PVDF) as binder and 90 wt.% of active material. The materials were mixed and pressed up to 450 kg for 15 min. The diameter of each electrode was 12 mm. Hence, each electrode had a geometric surface area of 1.13 cm<sup>2</sup>. The total electrode weight used for the measurements was about 30 mg. The electrodes were dried overnight before the cell was assembled. An aqueous solution of 1 M sulphuric acid was used as electrolyte, and so gold disks were used as current collectors in order to eliminate parasitic reactions. Glass fibre disks were employed as separators.

The electrochemical tests were performed in a Swagelok<sup>®</sup> cell, commonly used for testing electrode materials in electrochemical capacitors. This consists of two tightly screwed cylinders that act as current collectors for the two electrodes, to ensure good electrical contacts and a high reproducibility of results.

The electrochemical measurements were conducted in a *Biologic* multichannel potentiostat. Voltammetry experiments at a scan rate of 1 to 50 mV.s<sup>-1</sup>, galvanostatic charge/discharge tests in a voltage range of 0 to 1 V and impedance spectroscopy tests from 100 KHz to 1 mHz were carried out to assess the electrochemical behaviour of the activated materials. The capacitance values were expressed in Farads (F) per mass of active material present in the lightest electrode.

## 3. Results and discussion

### 3.1. Chemical characterization

The activation yields for the KOH-activated samples were rather similar for all temperatures studied, about 75%, whereas the yields for the NaOH-activated samples were in all cases ~ 65%.

The elemental composition of the activated carbons obtained in this study is shown in Table 1. It can be observed that, for both series, the oxygen content is significantly higher at lower activation temperatures. In order to clarify these results, both the KOH- and the NaOH-activated samples were characterized by TPD. Figs. 1 and 2 show the TPD profiles corresponding to the studied samples.

The surface oxygen groups on the carbon materials decompose upon heating, producing CO and CO<sub>2</sub> at different temperatures. It is known that CO<sub>2</sub> evolves at low temperatures as a consequence of the decomposition of acidic groups such as carboxylic groups, anhydrides or lactones<sup>17,18,19,20</sup>. The evolution of CO occurs at higher temperatures and is originated by the decomposition of basic or neutral groups such as phenols, ethers and carbonyls<sup>17,18,19,20</sup>.

The results of TPD ( Table 2) indicate that, in both series, the amount of CO evolved was larger than that of CO<sub>2</sub>. They also show that the lower the carbonization temperature, the greater the amount of oxygen groups. The decrease in the amount of CO and CO<sub>2</sub> evolved with the carbonization temperature is due to the increase in the extent of activation with the rise in temperature, according to equations (1) and (2). This means that, during activation higher intrapore hydrogen concentrations are formed, which destabilize and react with the oxygen surface groups<sup>21</sup>.

Moreover, the samples chemically activated with NaOH have a higher CO- and CO<sub>2</sub>-type group content than the KOH activated samples. These results are consistent with the data obtained by elemental analysis.

### 3.2. Porosity characterization

The N<sub>2</sub> adsorption isotherms obtained at 77 K for the KOH and the NaOH activated carbons are presented in Fig. 3. All the samples exhibit Type I isotherms according to the IUPAC classification<sup>13</sup>. This is characteristic of microporous solids, there being a sharp increase in the amount of nitrogen adsorbed at low relative pressures until a plateau is formed.

The parameters of the porous texture of both series of activated carbons calculated from the isotherms are presented in Tables 3 and 4.

It is interesting to note that the capacity of the samples activated with NaOH to adsorb nitrogen is hardly affected by the reduction in carbonization temperature. The BET surface area of these samples is around  $920 \text{ m}^2\cdot\text{g}^{-1}$  for all the temperatures tested. In the case of samples activated with KOH, a slight decrease in micropore surface is observed with decreasing carbonization temperature, from  $1636 \text{ m}^2\cdot\text{g}^{-1}$  for  $700^\circ\text{C}$  to  $1547 \text{ m}^2\cdot\text{g}^{-1}$  for  $600^\circ\text{C}$ ). Moreover, KOH activation can give rise to higher microporous materials under the same experimental conditions than NaOH activation.

It can also be seen from Fig. 3 that the isotherms of the NaOH-samples show a steady increase in nitrogen adsorption at higher pressures, and some hysteresis in the desorption branch, which is indicative of the presence of mesopores. This is consistent with the data obtained from the isotherms. In both series, it can be seen that the samples activated with NaOH have a higher mesopore volume than the KOH-activated samples, as one might expect from the shape of the isotherms. In general terms, the higher the carbonization temperature, the higher the mesopore volume in both series of samples.

### 3.3. Electrical conductivity

The activated carbons obtained at the higher temperatures show the best conductivity as shown in Figure 4. This increase in electrical conductivity upon activation occurs because activation removes the most disorganized parts of the precursor<sup>23</sup>. The porous carbons with the highest conductivity are those prepared with NaOH as activating agent.

### 3.4. Electrochemical properties

Table 5 contains the specific capacitance values estimated from the galvanostatic discharge at a constant current intensity of  $2 \text{ mA}$  (this corresponds to a current of about  $65 \text{ mA}\cdot\text{g}^{-1}$ ).

To calculate the specific capacitance ( $\text{F}\cdot\text{g}^{-1}$ ) from the galvanostatic experiments, the values of current applied ( $\text{mA}$ ) are multiplied by the discharge time ( $\text{s}$ ). The charge ( $q$ ) obtained is then divided by the range of voltage ( $\text{V}$ ) in which the capacitor is discharged. Taking into account the two electrode system, the capacitance of a single electrode is obtained multiplying the above result by two and dividing by the

mass of the smaller electrode. Capacitance can be related to the mass of the electrode or to the mass of the active material. In our case, capacitance is always expressed in Farads per active carbon material. In order to calculate from the cyclic voltammetry measurements, the capacitive current (A) is divided by the scan rate ( $\text{V.s}^{-1}$ ). The specific capacitance of a single electrode is  $C = 2 C_{\text{cell}}/\text{mass}$  in the active material of the smallest pellet.

Figure 5 shows the dependence of the specific capacitance values on the current density for both series of activated samples. The galvanostatic experiments showed that activation with KOH at lower temperature leads to specific capacitance values that are highly dependent on current density. In fact, for the sample activated at 700 °C the capacitance values decrease with the increase in current density (in the range studied) by only 40%, while this reduction is over 90% for the other two carbons (Table 5). However, the samples activated with NaOH show a rather different behaviour. Capacitance decreases with current density to a similar extent for all the samples. Moreover, for both series of activated carbons, the sample with the highest capacitance at 2 mA is not the sample with the highest BET surface area. Therefore other factors, apart from the surface area, must be contributing to the enhancement of capacitance.

Figure 6 shows the voltammogram profiles of all the activated samples. Samples KOH-650 and KOH-600 show a marked deviation from the ideal rectangular shape typical of cyclic voltammograms. However, samples activated with NaOH exhibit a quasi-rectangular shape in the voltammograms.

The differences between the two series may be due to the accessibility of porous network to the ions or to the type of chemical reactions occurring on the carbon surface. For all the samples studied, the average pore size was higher than 0.7 nm, while the ions used for this study had a Stokes radius lower than 0.24 nm (radius for the solvated species). Therefore, the problem of accessibility of the ions must be discarded as the reason for the different behaviours, as demonstrated elsewhere for aqueous solutions<sup>22</sup>. Therefore, only differences in faradic contribution can explain the divergent behaviours.

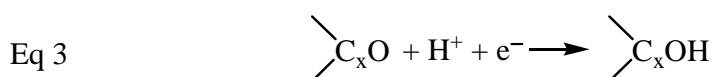
Cyclic voltammetry in a three-electrode configuration is an excellent technique for studying the presence of pseudocapacitive phenomena. Materials with pseudocapacitance show redox peaks related



to electron transfer reactions. The voltammograms in Figure 7 show the redox processes corresponding to samples KOH-650 and KOH-700. It should be noted that these redox reactions occur both in the cathodic and anodic regions, which means that capacitance is used in the symmetric cell.

For a deeper understanding of the influence of the oxygen functionalities on the capacitance values, we tried to correlate the specific capacitance (capacitance divided by the BET surface area) with the amount of surface oxygen groups desorbed as CO (also divided by the BET surface area too)<sup>23</sup> (Figure 8). An excellent correlation between specific capacitance and the amount of CO-type groups was found, indicating that these oxygen groups make a positive contribution to the capacitance of the porous carbons, as reported.<sup>23,24,25,26,27</sup>

The reason for the positive contribution to capacitance is either due to the improved wettability of the carbon material by the electrolyte, especially in the case of aqueous solutions, as a result of which the ions have better access to microporosity, or to the faradaic process involving oxygen groups that contribute to pseudocapacitance<sup>23</sup>. These oxygen surface groups are mainly hydroxyl, carbonyl or quinone complexes which can undergo through the well-known mechanism for the quinone/hydroquinone redox pair (Eq 3).



It has been suggested that oxygen functionalities are detrimental to the behaviour of supercapacitors as charge and discharge voltages may alter the surface oxygen groups, producing a loss in capacitance<sup>28</sup>. All of the capacitors were cycled in a galvanostatic regime of 8.84mA.cm<sup>-2</sup> (270 mA.g<sup>-1</sup>) in order to assess their durability. A good cycling behaviour was obtained for NaOH-samples and for KOH-700, with a reduction in the capacitance values of only about 17% after 6000 cycles. On the contrary, the long-term cycling for KOH-650 and KOH-600 was rather poor, with a reduction of about 60% and 75%, respectively, after 6000 cycles. For these samples, the large contribution of pseudocapacitance negatively affects the long-term behaviour of the supercapacitor, as expected<sup>29</sup>

The different behaviour of the capacitance of the activated samples on the current density may also be related to their differences in electrical conductivity. As can be seen from the impedance spectra (Fig. 9), samples activated with KOH at lower temperatures show a large semicircle in the mid-high frequency zone, which is related to the high intrinsic electrical resistance of the activated carbon<sup>30</sup>, and the presence of faradaic reactions. This resistance results in a high kinetic dependence on faradaic phenomena with current density. However, the NaOH-activated carbons impedance spectra do not show a semicircle in the mid-high frequency zone, which indicates a better resistive behaviour of the material. This is consistent with the ohmic drop obtained in the electrochemical analysis (0.5 V for the ohmic drop in the charge-discharge test for the NaOH-samples, and ~ 4 V for KOH-650 and KOH-600).

#### **4. Conclusions**

The TPD results showed that, at the lower activation temperatures, samples activated with NaOH have a higher oxygen content than those activated with KOH.

The porosity characterization results showed that all of the activated carbons produced are essentially microporous. KOH activation produces highly microporous materials, whereas when NaOH is used as activating agent, a material with a higher mesopore volume is produced. For both the NaOH and KOH series, it was found that the BET surface area increases with temperature.

The influence of the activation temperature on the electrochemical characteristics of the KOH- and NaOH-activated carbons is rather different. With NaOH as activating agent, the activated carbons show a similar electrochemical behaviour at all the activation temperatures. However, the samples activated with KOH at temperatures lower than 700 °C displayed a strong resistance due to the high pseudofaradaic contribution, resulting in an electrochemical behaviour that is highly dependent on the current density. The results show that CO-type oxygen groups make a positive contribution to capacitance, a good correlation being found between specific capacitance and this particular type of oxygen group.

The marked deviations in capacitive behaviour with current density for the KOH-650 and KOH-600 samples indicate that electrical conductivity is an important parameter in double layer capacitor performance. The electrical conductivity tests showed that the higher the activation temperature, the higher the conductivity obtained.

### **Acknowledgment**

This work was supported by the MICIN (Project MAT2007-61467). Silvia Roldán thanks MICIN for a FPI predoctoral grant.

### **REFERENCES**

- [1] Teng, H.; Lin, H. C. *Am. Inst. Chem. Eng. J.*, **1998**; 44 (5), 1170-1177.
- [2] Molina-Sabio, M; Rodríguez-Reinoso, F. *Colloids and Surfaces* **2044**, 241, 15-25.
- [3] Illán-Gómez, M. J.; García-García, A.; Salinas-Martínez de Lecea, C.; Linares-Solano, A. *Energy Fuels* **1996**, 10, 1108-1114.
- [4] Lozano-Castelló, D; Lillo-Ródenas, M. A.; Cazorla-Amorós, D.; Linares-Solano, A. *Carbon* **2001**, 39, 741-749.
- [5] Lillo-Ródenas, M. A.; Lozano-Castelló, D.; Cazorla-Amorós, D.; Linares-Solano, A. *Carbon* **2001**, 39, 751-759.
- [6] Teng, H.; Hsu, L. *Ind. Eng. Chem. Res.* **1999**, 38, 2947-2953.
- [7] Evans, M. J. B.; Halliop, E.; MacDonald, J. A. F. *Carbon* **1999**, 37, 269-274.
- [8] Hayashi, J.; Watkinson, A. P.; Teo K. C.; Takemoto, S.; Muroyama, K. *Coal Sci* **1995**, 1, 1121-1124.

- [9] Díaz-Teran, J.; Nevskaja, D. M.; Fierro, J. L. G.; López-Peinado, A. J.; Jerez, A. *Micropor. Mesopor. Mat.* **2003**, 60, 173-181.
- [10] Lillo-Ródenas, M. A.; Cazorla-Amorós, D.; Linares-Solano A. *Carbon* **2003**, 41, 267-275.
- [11] Lillo-Ródenas, M. A.; Cazorla-Amorós, D.; Linares-Solano, A.; Béguin, F.; Clinard, C.; Rouzaud, J. N. *Carbon* **2004**, 42, 1305-1310.
- [12] Lillo-Ródenas, M. A.; Juan-Juan, J.; Cazorla-Amorós, D.; Linares-Solano, A. *Carbon* **2004**, 42, 1371-1375.
- [13] Sing, K. S. W.; Everett, D.H.; Haul, R.A.W.; Moscou, L.; Pierotti P.A.; Rouquerol, J. *Pure Appl. Chem.* 1985, 57, 603-619.
- [14] Dubinin, M. M. in: *Porosity in carbons*; J. W. Patrick (Ed.), Edward Arnold, London, 1995; chapter 3.
- [15] Stoeckli, H. F. in: *Porosity in carbons*; J. W. Patrick (Ed.), Edward Arnold, London, 1995; chapter 3.
- [16] L. J. Van der Pauw, *Philips Technical Review* 20 (1958) 220.
- [17] Kinoshita, K. *Carbon: Electrochemical properties and Physicochemical properties*; New York, Wiley, 1998.
- [18] Rodríguez-Reinoso, F.; Molina-Sabio, M. *Adv. Coll. Inter. Sci.* **1998**, 76-77 895-902.
- [19] Román-Martínez, M. C.; Cazorla-Amorós, D.; Linares-Solano, A.; Salinas-Martínez de Lecea, C. *Carbon* **1993**, 31, 895-902.
- [20] Figueredo J. L.; Pereira, M. F. R.; Freitas, M. M. A.; Órfao, J. J. M. *Carbon* **1999**, 37, 1379-1389.

- [21] Calo, J. M.; Cazorla-Amoros, D.; Linares-Solano, A.; Roman-Martínez, M. C.; Salinas-Martínez de Lecea, C. *Carbon*, **1997**, 35, 543-554.
- [22] Ruiz, V.; Blanco, C.; Santamaría, R.; Juárez-Galán, J. M.; Sepúlveda-Escribano, A.; Rodríguez-Reinoso, F. *Microporous Mesoporous Mater.* **2008**, 110, pp 431-435.
- [23] Bleda-Martínez, M. J.; Maciá-Agulló, J. A.; Lozano-Castelló, D.; Morallón, E.; Cazorla-Amorós, D.; Linares-Solano, A. *Carbon* **2005**, 43, 2677-2684.
- [24] Hsieh, C.; Teng, H. *Carbon* **2002**, 40, 667-674.
- [25] Okajima, K.; Ohta, K.; Sudoh, M. *Electrochim Acta* **2005**, 50, 2227-2231.
- [26] Centeno, T. A.; Hahn, M.; Fernández, J. A.; Kötz, R.; Stoeckli, F. *Electrochemistry Communications* **2007**, 9, 1242-1246.
- [27] Centeno, T. A.; Stoeckli, F. *Electrochimica Acta* **2006**, 52 (2), 560-566.
- [28] Kierzek, K.; Frackowiak, E.; Lota, G.; Gryglewicz, G.; Machnikowski, J. *Electrochimica Acta* **2004**, 49, 515-523.
- [29] Kierzek, K.; Frackowiak, E.; Lota, G.; Gryglewicz, G.; Machnikowski, J. *Electrochimica Acta* **2004**, 49, 515-523.
- [30] Andrieu, X.; Crépy, G.; Josset, L. *Contribution at the 3<sup>er</sup> international seminar: On Double layer Capacitors and Similar Energy Storage Devices*; Florida Educational Seminar Editors, Deerfield Beach FL, USA, December 1993, 3-5.

## FIGURE CAPTIONS

Fig 1. TPD curves corresponding to CO desorption in KOH- and NaOH-activated samples.

**Fig 2.** TPD curves corresponding to CO<sub>2</sub> desorption in KOH- and NaOH-activated samples.

**Figure 3.** Nitrogen adsorption isotherms of carbons activated with: a) KOH, b) NaOH.

**Figure 4.** Electrical conductivity values at different pressures.

**Figure 5.** Specific capacitance values vs. current densities for: a) KOH activated carbons, b) NaOH activated carbons.

**Figure 6.** Cyclic voltammograms in a two-electrode cell for: a) KOH and b) NaOH activated carbons.

**Figure 7.** Cyclic voltammograms in a three-electrode cell for: a) KOH and b) NaOH activated carbons.

**Figure 8.** Capacitance / BET surface area v.s CO content / BET surface area for: a) KOH-activated samples and b) NaOH-activated samples.

**Figure 9.** Impedance spectroscopy plot. Extended high frequency region of: a) KOH-activated carbons, b) NaOH-activated carbons.

## TABLE CAPTIONS

**Table 1.** Elemental composition of activated carbons.

**Table 2.** TPD analysis for the activated carbons.

**Table 3.** Textural parameters of carbons activated with KOH.

**Table 4.** Textural parameters of carbons activated with NaOH.

**Table 5.** Specific capacitance values of the KOH and NaOH-activated carbons estimated by galvanostatic discharge at 2 mA and capacitance decrease values with current density.

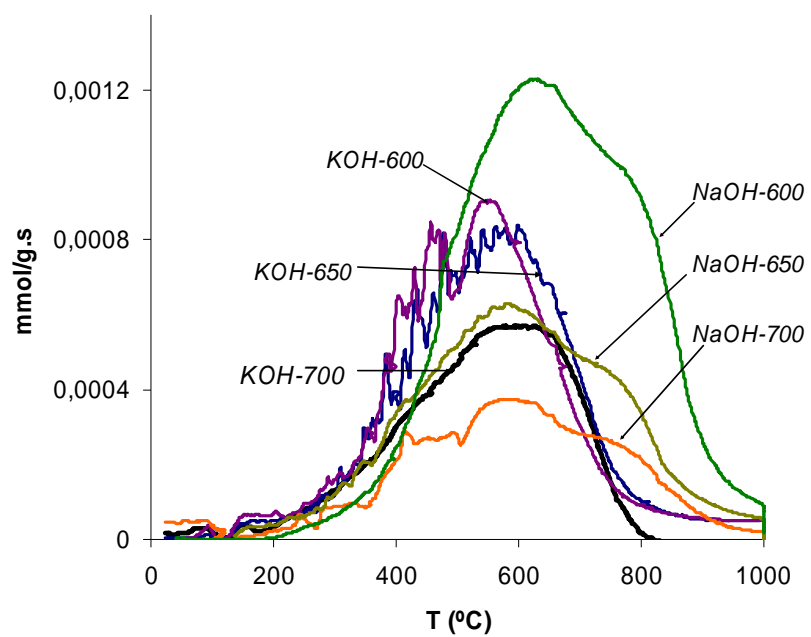
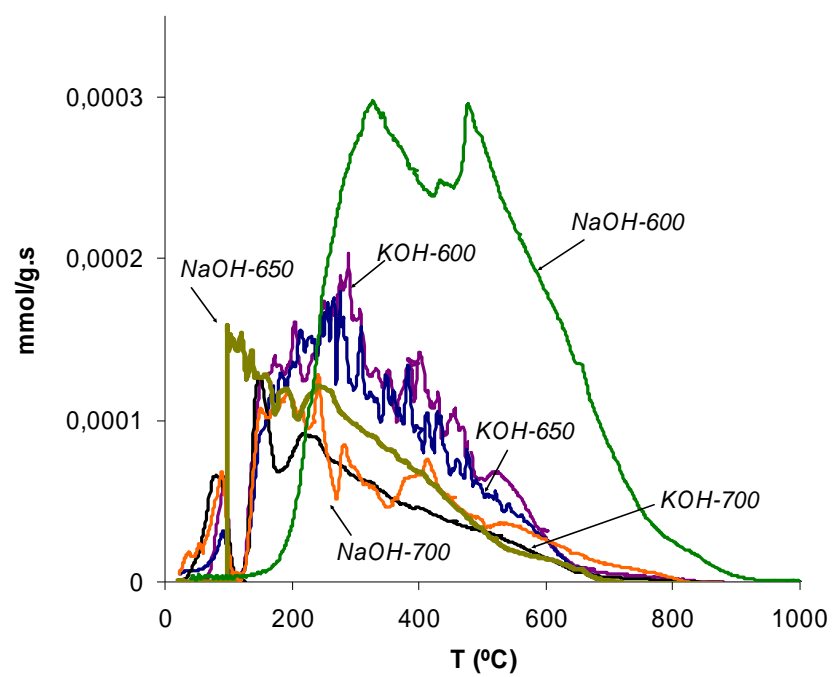


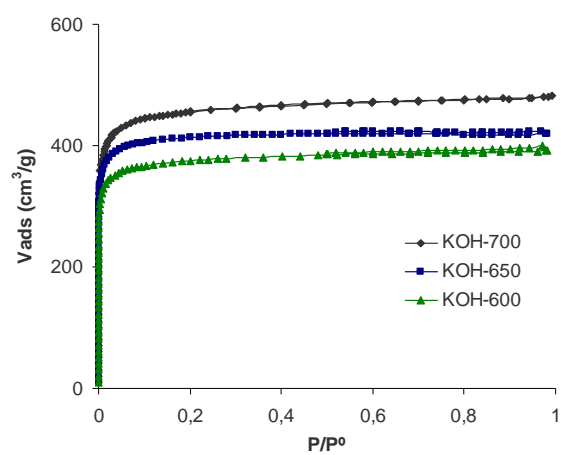
Fig 1. TPD curves corresponding to CO desorption in KOH- and NaOH-activated samples.





**Fig 2.** TPD curves corresponding to CO<sub>2</sub> desorption in KOH- and NaOH-activated samples.

a)



b)

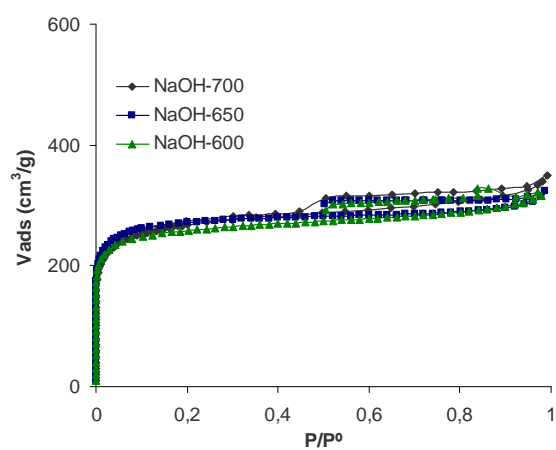


**Figure 3.** Nitrogen adsorption isotherms of carbons activated with: a) KOH, b) NaOH.

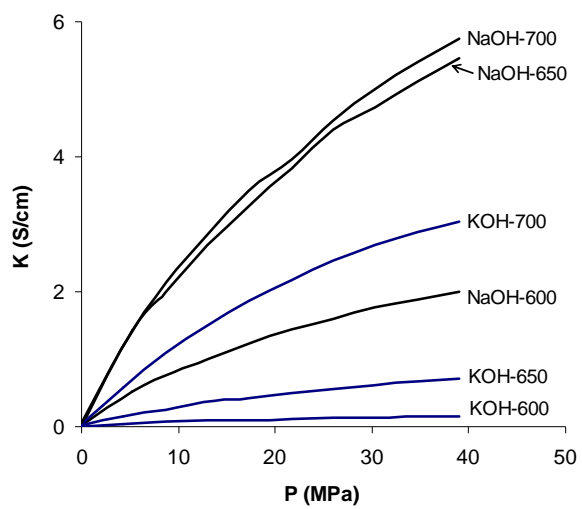


**Figure 4.** Electrical conductivity values at different pressures.

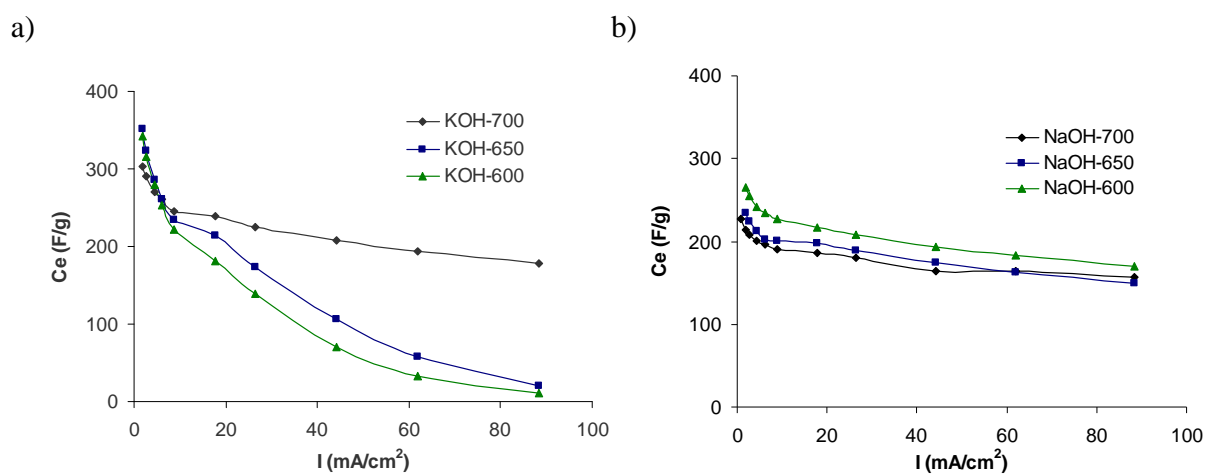


**Figure 5.** Specific capacitance values vs. current densities for: a) KOH activated carbons, b) NaOH activated carbons.

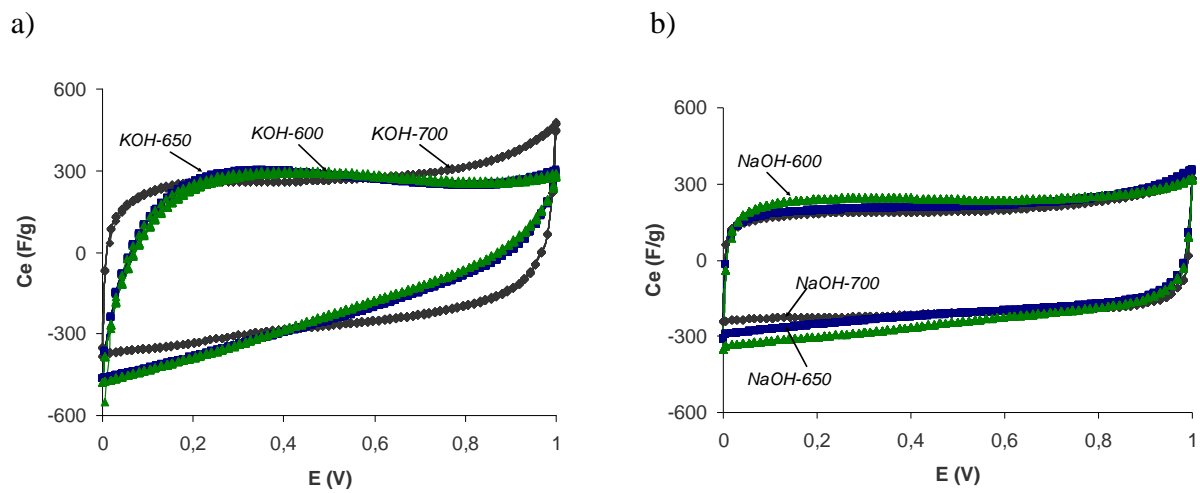
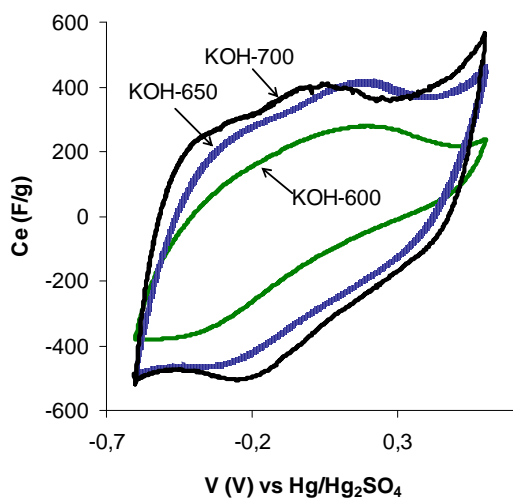


**Figure 6.** Cyclic voltammograms in a two-electrode cell for: a) KOH and b) NaOH activated carbons.

a)



b)

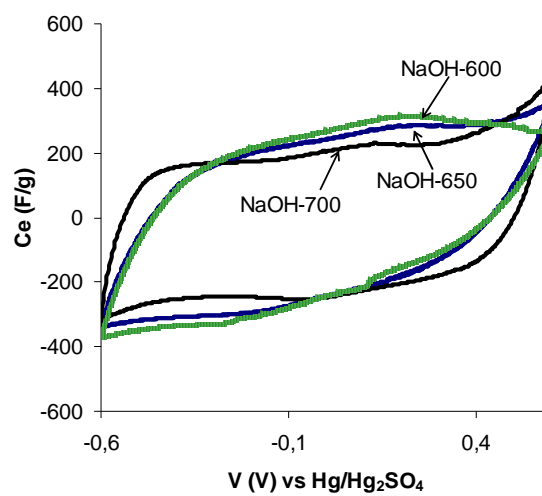
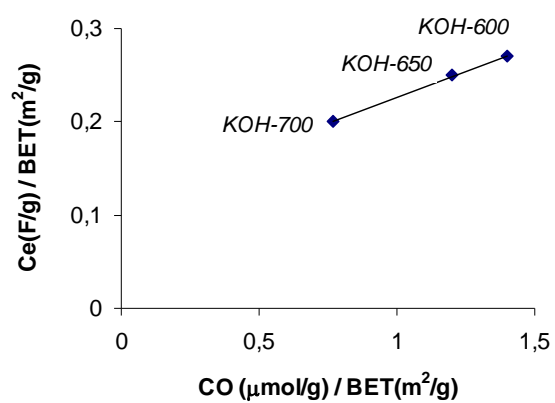


**Figure 7.** Cyclic voltammograms in a three-electrode cell for: a) KOH and b) NaOH activated carbons.

a)



b)

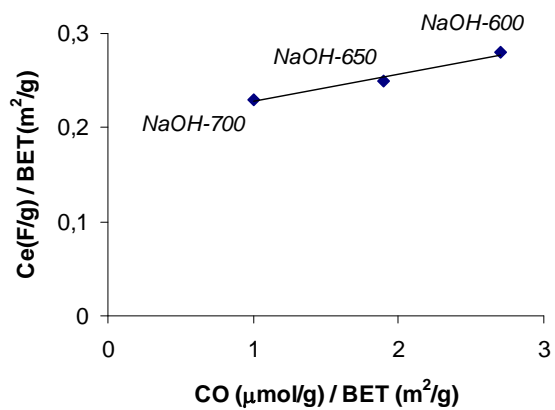
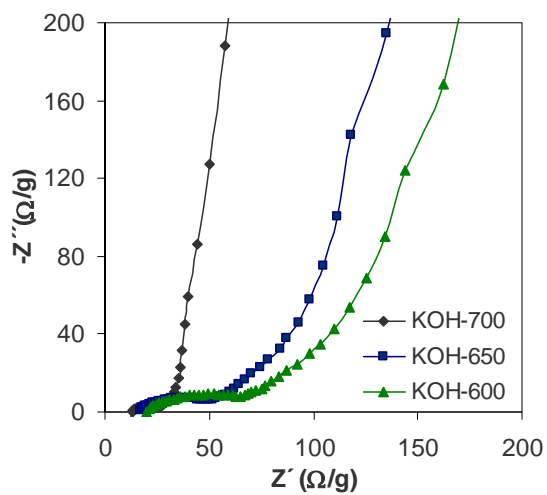


**Figure 8.** Capacitance / BET surface area v.s CO content / BET surface area for: a) KOH-activated samples and b) NaOH-activated samples.

a)



b)

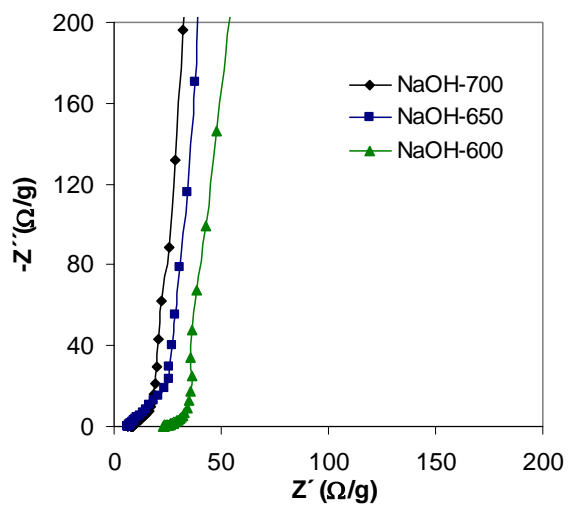


**Figure 9.** Impedance spectroscopy plot. Extended high frequency region of: a) KOH-activated carbons, b) NaOH-activated carbons.



**Table 1.** Elemental composition of activated carbons.

Sample	C (wt.% )	H (wt.% )	N (wt.% )	S (wt.% )	O (wt.% )	Sample	C (wt.% )	H (wt.% )	N (wt.% )	S (wt.% )	O (wt.% )
KOH-700	92.24	0.77	0.89	0.09	6.00	NaOH-700	95.34	0.55	0.52	0.07	3.52
KOH-650	89.71	1.25	1.20	0.15	7.68	NaOH-650	92.91	0.67	0.54	0.07	5.81
KOH-600	89.78	1.52	1.22	0.18	7.30	NaOH-600	88.96	0.99	0.59	0.10	9.35

**Table 2.** TPD analysis for the activated carbons.

Sample	CO (mmol.g <sup>-1</sup> )	CO <sub>2</sub> (mmol.g <sup>-1</sup> )	Sample	CO (mmol.g <sup>-1</sup> )	CO <sub>2</sub> (mmol.g <sup>-1</sup> )
KOH-700	1.14	0.18	NaOH-700	0.96	0.21
KOH-650	1.73	0.3	NaOH-650	1.75	0.44
KOH-600	1.73	0.33	NaOH-600	2.5	0.8

**Table 3.** Textural parameters of carbons activated with KOH.

Sample	$S_{\text{BET}}$ ( $\text{m}^2/\text{g}$ )	$S_{\text{mic}}$ ( $\text{m}^2/\text{g}$ )	$E_0$ ( $\text{KJ/mol}$ )	$L_0$ ( $\text{nm}$ )	$V_{\text{total}}$ ( $\text{cm}^3/\text{g}$ )	$V_{\text{mic}}$ ( $\text{cm}^3/\text{g}$ )	$V_{\text{meso}}$ ( $\text{cm}^3/\text{g}$ )
KOH-700	1480	1636	24.55	0.8	0.75	0.67	0.07
KOH-650	1397	1624	25.35	0.77	0.66	0.63	0.03
KOH-600	1272	1547	26.04	0.74	0.61	0.57	0.04

$S_{\text{BET}}$ , BET apparent area       $V_{\text{total}}$ , total volume of pores  
 $S_{\text{mic}}$ , microporous surface       $V_{\text{mic}}$ , micropore volume  
 $E_0$ , characteristic energy       $V_{\text{mes}}$ , mesopore volume  
 $L_0$ , average pore width

**Table 4.** Textural parameters of carbons activated with NaOH.

Sample	$S_{\text{BET}}$ ( $\text{m}^2/\text{g}$ )	$S_{\text{mic}}$ ( $\text{m}^2/\text{g}$ )	$E_0$ ( $\text{KJ/mol}$ )	$L_0$ ( $\text{nm}$ )	$V_{\text{total}}$ ( $\text{cm}^3/\text{g}$ )	$V_{\text{mic}}$ ( $\text{cm}^3/\text{g}$ )	$V_{\text{meso}}$ ( $\text{cm}^3/\text{g}$ )
NaOH-700	922	804	23.51	0.9	0.54	0.36	0.18
NaOH-650	936	886	24.05	0.85	0.50	0.38	0.12
NaOH-600	918	868	24.13	0.85	0.49	0.37	0.12

$S_{\text{BET}}$ , BET apparent area       $V_{\text{total}}$ , total volume of pores  
 $S_{\text{mic}}$ , microporous surface       $V_{\text{mic}}$ , micropore volume  
 $E_0$ , characteristic energy       $V_{\text{mes}}$ , mesopore volume  
 $L_0$ , average pore width

**Table 5.** Specific capacitance values of the KOH and NaOH-activated carbons estimated by galvanostatic discharge at 2 mA and capacitance decrease values with current density.

Sample	Specific capacitance (F/g)	Capacitance decrease with current density (%)
KOH-700	302.4	41,0
KOH-650	350.9	96.9
KOH-600	341.9	91.4
NaOH-700	227.3	20.4
NaOH-650	234.8	36.4
NaOH-600	265.3	35.9